horticulturae

MDPI

Article

Alginate Oligosaccharide Coordinately Modulates Endogenous Phytohormone Profiles to Enhance Tomato Growth

Yun Li, Jianxia Wang, Kai Fan, Lingru Guo, Leiping Hou, Yanxiu Miao, Meihua Sun, Yaling Li * and Longqiang Bai *

College of Horticulture, Shanxi Agricultural University, Jinzhong 030801, China; sxndly412@126.com (Y.L.); x13176262997@163.com (J.W.); fanxiaopang1999@163.com (K.F.); 17839197266@163.com (L.G.); sxndhlp@126.com (L.H.); miaoyanxiu@163.com (Y.M.); sunmeihua19@163.com (M.S.)
* Correspondence: yalingli1988@163.com (Y.L.); lqbai@sxau.edu.cn (L.B.)

Abstract: Alginate oligosaccharides (AOSs) have been shown to be effective in enhancing crop growth. However, their functions in horticulture crops and growth-promoting mechanisms remain insufficiently characterized. This study employed pot cultivation experiments to investigate the effects of AOS root drenching (0, 15, 30, 45 mg·L^{-1}) on tomato (*Solanum lycopersicum* L.) seedling growth, photosynthetic performance, and phytohormone accumulation. The results showed that AOS promoted the leaf count per plant, leaf area of the youngest fully expanded leaves, shoot and root dry mass, chloroplast pigment contents and photosynthetic rate of tomato seedlings. And the 30 mg·L^{-1} treatment consistently showed optimal efficacy, in which tomato seedlings also exhibited a significantly longer total root length, a larger root surface area and a greater number of root tips compared to the control. Phytohormone profiling revealed that AOS differentially regulated shoot/root phytohormones as follows: increasing auxins/cytokinins (CKs)/GA_{19} content in shoots and Indole-3-acetic acid (IAA)/CKs/1-aminocyclopropane-1-carboxylic acid (ACC) content in roots, while decreasing root Jasmonic acid (JA)/5-deoxystrigol (5DS) contents. Finally, these findings demonstrate that AOS enhances tomato growth by coordinately reprogramming phytohormone homeostasis.

Keywords: AOS; tomato; plant growth; photosynthetic rate; phytohormone

check for updates

Academic Editor: Piotr Salachna

Received: 21 April 2025
Revised: 20 May 2025
Accepted: 22 May 2025
Published: 24 May 2025

Citation: Li, Y.; Wang, J.; Fan, K.; Guo, L.; Hou, L.; Miao, Y.; Sun, M.; Li, Y.; Bai, L. Alginate Oligosaccharide Coordinately Modulates Endogenous Phytohormone Profiles to Enhance Tomato Growth. *Horticulturae* **2025**, *11*, 580. https://doi.org/10.3390/horticulturae11060580

Copyright: © 2025 by the authors. Licensee MDPI, Basel, Switzerland. This article is an open access article distributed under the terms and conditions of the Creative Commons Attribution (CC BY) license (https://creativecommons.org/licenses/by/4.0/).

1. Introduction

While agrochemicals and fertilizers have long been used to boost agricultural productivity, their adverse environmental and health consequences are now prompting a global shift away from chemical-dependent farming practices [1]. To promote sustainable agriculture and reduce reliance on chemical fertilizers, governments worldwide have implemented stringent agro-environment policies, including the European Union's 'Nitrates Directive' and China's 'Action Plan for Zero Growth in Fertilizer Use by 2020' [2,3]. Biostimulants represent an eco-friendly innovation that enhances agricultural sustainability by reducing dependence on synthetic agrochemicals. These biological agents enhance nutrient use efficiency by promoting plant growth and development, boosting crop productivity and improving stress tolerance—all while reducing reliance on fertilizers and pesticides [4]. Alginate oligosaccharides (AOSs), produced from sodium alginate through enzymatic degradation, ionization radiation or other methods, represent a novel class of highly biodegradable and eco-friendly plant biostimulants [5,6]. AOSs are composed of a set of β-D-mannuronic acid (ManA) and α-L-guluronic acid (GulA) residues [5–7] and have been demonstrated to positively regulate mineral nutrient absorption and utilization,

plant growth, synthesis of secondary metabolites and even stress tolerance in many crops, such as fennel (*Foeniculum vulgare* Mill.) [8], *Artemisia annua* L. [9], *Mentha arvensis* L. [10], *Eucalyptus citriodora* Hook [11], *Vigna radiata* L. [12], barley (*Hordeum vulgare* L.) [7], Chinese cabbage (*Brassica campestris* L. *var. utilis* Tsen et Lee) [13] and wheat (*Triticum aestivum* L.) [14]. Most recently, AOSs derived from two Moroccan brown seaweed species were found to enhance phenolic metabolism in the roots and leaves of tomato seedlings while stimulating their natural defense mechanisms [15]. Excessive fertilizer use remains a persistent issue in China's intensive protected horticulture production systems [16]. However, the function of AOSs in protected horticulture crops remains poorly understood. Moreover, the mechanistic basis through which AOSs regulate plant growth and metabolic processes remains to be elucidated.

Phytohormones regulate a wide range of plant growth and developmental processes, as well as plant interactions with the environment. Previous studies have shown that phytohormones play important roles in AOS-regulated plant physiological processes. AOS regulates rice root formation and growth by accelerating auxin biosynthesis and transport [17]. In barley (*Hordeum vulgare* L.), AOS was also shown to upregulate the expression of auxin response factors [7]. Furthermore, AOS was proposed to enhance drought stress resistance in an ABA-dependent manner in wheat (*Triticum aestivum* L.) [18] and cucumber (*Cucumis sativus* L.) [19]. Additionally, Zhang et al. [20] found that AOS increased salicylic acid (SA) levels and enhanced resistance to *Pst* DC3000 in wild-type *Arabidopsis thaliana* but not in the SA-deficient mutant *sid2*. This suggested that AOS-induced disease resistance depends on the SA signaling pathway.

Previous studies have been limited to investigating the roles of individual hormones in mediating the effects of AOS on plant growth or stress responses. It is well known that crosstalk among different hormones frequently occurs in modulating plant growth and environmental adaptation. To better understand the growth-promoting mechanism of AOS, simultaneous quantification of multiple phytohormones is necessary. However, research on multi-hormonal profiles in AOS-treated plants remains scarce. In the reported literature, Zhang et al. [13] quantified four phytohormones—indole-3-acetic acid (IAA), *trans*-zeatin riboside (tZR), gibberellin A_3 (GA_3) and abscisic acid (ABA)—using enzyme-linked immunosorbent assay (ELISA) in AOS-treated flowering Chinese cabbage. Nonetheless, existing data cannot sufficiently explain AOSs' phytohormonal regulation of crop growth and metabolism.

Tomato (*Solanum lycopersicum* L.) is one of the most widely cultivated crops in protected horticulture worldwide. Previous studies have indicated that the optimal application concentration of AOS varies depending on crop species, generally ranging from 10 to 75 mg·L^{-1} [12,14]. This study aims to investigate the effects of root-applied AOS at varying concentrations on tomato seedling growth and determine the optimal application dosage. Meanwhile, LC-MS/MS analysis was employed to acquire comprehensive profiling data of AOS-modulated phytohormone metabolomes. The findings of this study provide both practical guidance for optimizing AOS application in protected horticulture systems and theoretical insights into the mechanisms whereby AOS regulates plant growth and development.

2. Materials and Methods

2.1. Experimental Materials

The tomato cultivar 'Zhongza 9' was used in this study. Seeds were first treated with hot water (50–55 °C) for 15 min, then germinated in darkness at 28 °C for 48 h after the water cooled to room temperature. Germinated seeds were sown in 72-cell seedling trays filled with a peat/vermiculite/perlite (2:1:1, *v*/*v*/*v*) growth substrate. Uniformly grown seedlings

with three true leaves were transplanted into pots (15 cm diameter × 15 cm height) containing the same substrate mixture. Plants in seedling trays received Hoagland nutrient solution every two days, while potted plants were irrigated every five days, continuing until slight drainage was observed from the container base. Seedlings were cultivated under natural light and temperature conditions in a solar greenhouse at Shanxi Agricultural University (37°25′42″ N, 112°35′11″ E). The AOS used in this study consisted of linear β-D-mannuronic acid and α-L-guluronic acid oligomers with a degree of polymerization below 20 (molecular weight < 5 kDa), produced by BZ Oligo Biotech Co., Ltd. (Qingdao, China) via enzymatic hydrolysis technology developed by Ocean University of China [6].

2.2. Experimental Design

The experiment comprised four AOS root drenching treatments with the following concentrations:

- Control: 0 $mg \cdot L^{-1}$ AOS
- A15: 15 $mg \cdot L^{-1}$ AOS
- A30: 30 $mg \cdot L^{-1}$ AOS
- A45: 45 $mg \cdot L^{-1}$ AOS

The four treatments were randomly assigned to experimental units in triplicate following a completely randomized design. Each replicate consisted of 50 tomato seedlings. AOS was dissolved in Hoagland nutrient solution and applied via root irrigation starting at 5 days after transplanting. Plants were irrigated every 5 days with 100 mL of Hoagland nutrient solution supplemented with the corresponding AOS concentration, for a total of four applications. On the 21st day after treatment initiation, plant growth traits and the net photosynthetic rate (Pn) were quantified. The youngest fully expanded leaves were collected for chloroplast pigment content estimation. The apical bud (defined as the stem region above the first unfolded leaf, containing the shoot apical meristem and young leaves) and the 3–4 cm root tip segment were collected for phytohormone profiling.

To analyze root architecture parameters of tomato seedlings, a supplementary pot (15 cm diameter × 15 cm height) experiment was conducted using coco coir as the growth substrate. Seedlings were divided into two treatment groups. One group was irrigated with Hoagland nutrient solution only (0 $mg \cdot L^{-1}$ AOS, control), the other group was irrigated with Hoagland solution supplemented with 30 $mg \cdot L^{-1}$ AOS (A30). Similarly, each treatment was replicated three times in a completely randomized arrangement. Plants received three applications (at 5-day intervals) of Hoagland solution (100 mL each pot) containing either AOS or no AOS. Root architecture analysis was performed on the 15th day after treatment initiation.

2.3. Measurement of Growth Parameters

Plant height was recorded as the vertical extent from the root–shoot junction to the apical bud using a meter stick. For dry mass (DM) quantification, harvested seedlings were separated into root and shoot fractions. Following three rinses with distilled water and surface drying with filter paper, samples were oven-dried with an initial 15 min deactivation at 105 °C, followed by drying at 80 °C to constant weight for biomass determination. Total leaf count per plant was determined by enumerating all expanded leaves, including the first unfolded leaf. The youngest fully expanded leaves were photographed, and their area was measured using LA-S plant leaf image analyzer software (Smart Lite Version, WSeen, Hangzhou, China).

2.4. Root Morphological Analysis

For root morphological analysis, excised roots were gently rinsed with water and scanned using an Epson Perfection V850 Pro scanner (Epson, Suwa, Nagano, Japan). Root morphological traits, including total root length, root diameter, total surface area and root tip count were analyzed with WinRHIZO root analysis software, version 2.0.3 (Regent Instruments, Québec, QC, Canada).

2.5. Chloroplast Pigments and Pn Measurements

Chloroplast pigment concentrations, including chlorophyll a (Chl a), chlorophyll b (Chl b) and carotenoids (Car), were quantified spectrophotometrically (UV-2600, Shimadzu, Kyoto, Japan) using 95% ethanol as the solvent, following the method of Sumanta et al. [21]. Pn of the youngest fully expanded leaves was measured using an LI-6400 portable photosynthesis system (LI-COR Biosciences, Lincoln, NE, USA).

2.6. Phytohormone Profiling

Phytohormone contents were quantified by MetWare Biotechnology Co., Ltd. (Wuhan, China) using the AB 6500+ QTRAP® LC-MS/MS platform [22].

2.7. Data Analysis

Statistical analyses were performed with the Data Processing System (DPS), version 12.01 (Refine, Hangzhou, China). Normality was assessed using the Shapiro–Wilk test. For analyses involving four groups, homogeneity of variance was evaluated with the Brown–Forsythe test. Data meeting normality and homoscedasticity assumptions were analyzed using one-way ANOVA, followed by LSD post hoc tests. For non-normally distributed data, the Kruskal–Wallis procedure in DPS 12.01 software was used for overall difference analysis, followed by pairwise comparisons. For two-group comparisons, normally distributed data were analyzed using Student's *t*-test, and statistical results were interpreted based on variance homogeneity testing. Non-normal data were examined using the Wilcoxon test. Data were visualized with GraphPad Prism version 9.0.0 (GraphPad Software Inc., San Diego, CA, USA).

3. Results

3.1. Effects of AOS Application on the Growth of Tomato Seedlings

After 21 days of treatment, AOS promoted the growth of tomato seedlings, with the optimal promoting effect observed at a concentration of 30 $mg \cdot L^{-1}$ (Figure 1). The A30 treatment significantly enhanced seedling growth parameters compared to the control, with increases of 14.31% in plant height, 21.95% in shoot dry mass (DM), and 20.26% in root DM ($p < 0.05$). Additionally, leaf count per plant was significantly higher in A30 than in the control (Figure 1c). The leaf area of the youngest fully expanded leaves under A30 treatment exhibited a 20.23% increase relative to the control (Figure 1d).

3.2. Effects of AOS Application on Chloroplast Pigment Contents and Photosynthetic Rate of Tomato Leaves

As shown in Figure 2, AOS application enhanced chloroplast pigment contents and Pn in tomato leaves. The Chl b content in A30 and A45 was significantly higher than in the control ($p < 0.05$). Among the four treatments, A30 showed the highest levels of Chl a, carotenoids and Pn.

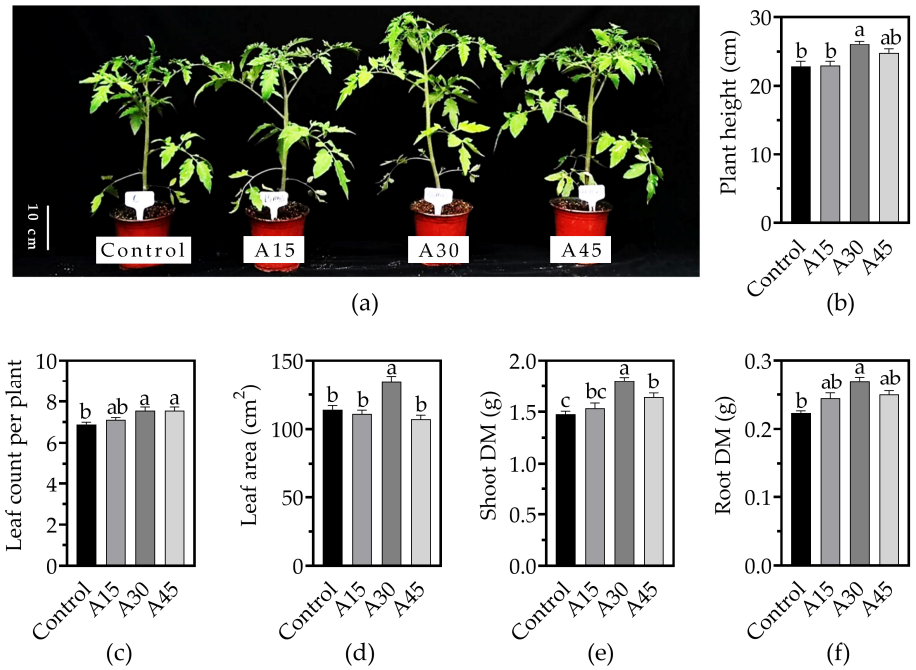


Figure 1. Effects of AOS on the growth of tomato seedlings. (**a**) The appearance of tomato seedlings. (**b**) Plant height of tomato seedlings. (**c**) Leaf count per plant. (**d**) Leaf area of the youngest fully expanded leaves. (**e**) Shoot dry mass (DM) of tomato seedlings. (**f**) Root DM of tomato seedlings. Values are means ± SE (n = 9). Data were analyzed using one-way ANOVA, followed by LSD post hoc tests (normally distributed data), or the Kruskal–Wallis test (non-normally distributed data). Different lowercase letters indicate significant differences at the 0.05 level.

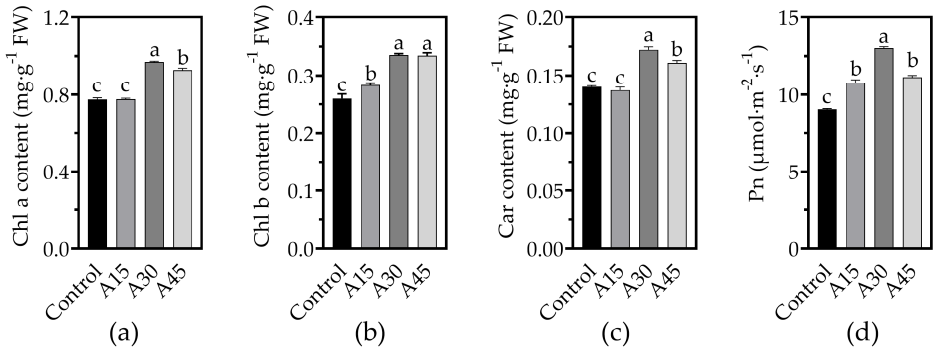


Figure 2. Effects of AOS on chlorophyll a content (**a**), chlorophyll b content (**b**), carotenoid content (**c**) and Pn (**d**) of tomato seedlings. Values are means ± SE (n = 9). Data were analyzed using one-way ANOVA, followed by LSD post hoc tests. Different lowercase letters indicate significant differences at the 0.05 level.

3.3. Effects of AOS Application on the Root Architecture Parameters of Tomato Seedlings

The results demonstrated that tomato seedlings grown under A30 treatment exhibited a significantly longer total root length (Figure 3a) and a larger root surface area (Figure 3c) compared to the control. However, no significant difference was observed in root diameter between A30 and the control. Additionally, the A30 treatment led to a greater number of root tips (Figure 3d), suggesting that AOS enhances lateral root development.

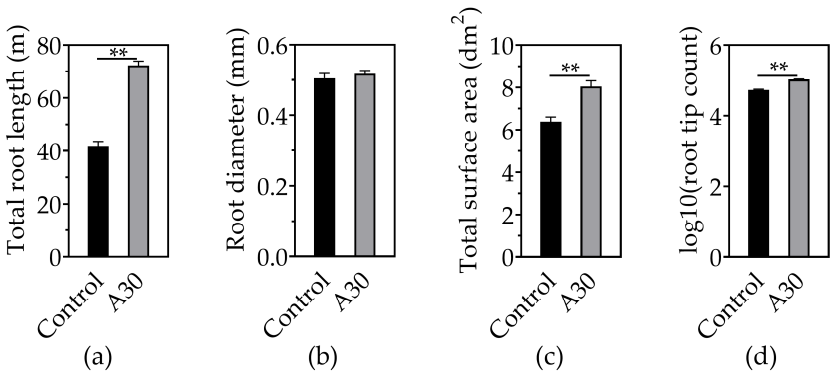


Figure 3. Total root length (**a**), average root diameter (**b**), total root surface area (**c**) and total root tips count (**d**) of tomato seedlings grown under control and A30 treatments for 15 days. Values are means ± SE (n = 9). Data were analyzed by Student's t-test. ** indicates a significant difference between the control and A30 at the 0.01 level.

3.4. Effects of AOS on Phytohormone Concentrations in Tomato Seedlings

As shown in Figure 4, our analysis detected 10 auxins and their derivatives in the investigated tomato tissues. Under A30 treatment, young leaves and roots exhibited a significant increase in IAA content compared to the control. No statistically significant differences were observed in IAA precursors (IBA, TRP, TAM and IAN) in young leaves or roots between the control and A30. The storage form of IAA, MeIAA, accumulated significantly in young leaves but showed no variation in roots. IAA-Val-Me displayed consistent levels in both tissues. IAA-Asp was exclusively detected in roots, with no treatment-induced differences in concentration. Two IAA catabolites, IAA-Val and IAA-Glc, were identified in young leaf tissues. Notably, A30 treatment led to a significant increase in IAA-Val content.

A total of 14 cytokinins (CKs) and their derivatives were detected in this study (Figure 5). Compared with the control, the content of tZ increased significantly in roots but showed no difference in young leaves. No significant differences were observed for iP or cZ (the low biological activity isomer) in either roots or young leaves. We identified six inactive CKs, which are involved in CK storage and transport, including four riboside types of CKs (iPR, cZR, 2MeScZR, pTR) and two O-linked glucosyl CKs (tZOG, cZROG). Compared to the control, Czr content significantly increased in A30 treatment in young leaves but decreased in roots, while 2MeScZR levels were significantly increased in roots. iPR and cZROG showed no changes in either tissue. pTR and tZOG were exclusively detected in young leaves, with tZOG showing significant accumulation under A30 treatment. Additionally, five N-glucosylated CK derivatives (iP7G, iP9G, cZ9G, pT9G and DHZ7G) were identified as products of the CK inactivation pathway. A30 treatment significantly increased root iP7G and iP9G levels compared to the control and exclusively elevated DHZ7G level in young leaves. cZ9G and pT9G were exclusively detected in tomato roots across both treatments, though without statistical significance.

Two precursors of bioactive GAs were detected in tomato tissues (Figure 6). GA_{15}, the precursor of bioactive GA_4, showed no significant differences in content between the control and A30 in both young leaves and roots. GA_{19}, which serves as the precursor for bioactive GA_1 and GA_3, was exclusively present in young leaves and exhibited a significant increase in A30 treatment.

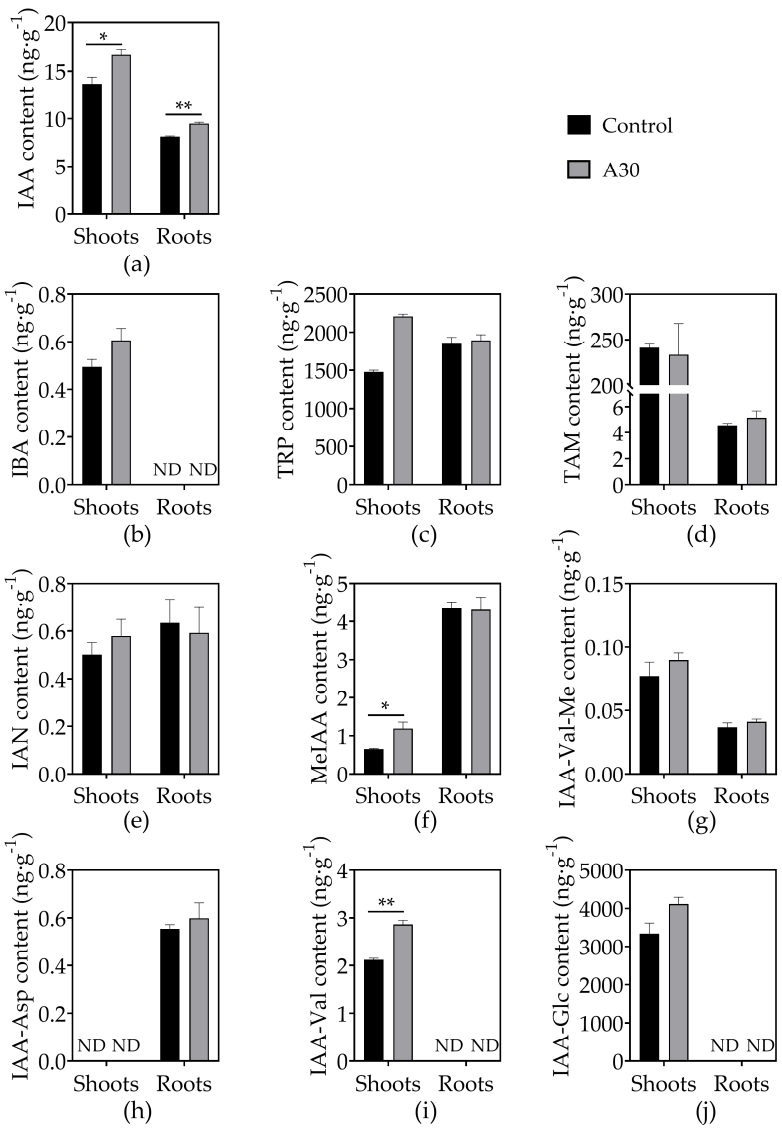


Figure 4. Contents of auxins and their derivatives in shoots and roots of tomato seedlings subjected to control and A30 treatments for 21 days. (**a**) IAA (Indole-3-acetic acid) content. (**b**) IBA (Indole-3-butyric acid) content. (**c**) TRP (L-tryptophan) content. (**d**) TAM (Tryptamine) content. (**e**) IAN (3-indoleacetonitrile) content. (**f**) MeIAA (Methyl indole-3-acetate) content. (**g**) IAA-Val-Me (Indole-3-acetyl-L-valine methyl ester) content. (**h**) IAA-Asp (Indole-3-acetyl-L-aspartic acid) content. (**i**) IAA-Val (Indole-3-acetyl-L-valine) content. (**j**) IAA-Glc (1-O-indol-3-ylacetylglucose) content. Values are means ± SE (n = 3). Data were analyzed using Student's t-test (normally distributed data), or the Wilcoxon test (non-normally distributed data). ND: not detected in the samples. * and ** indicate significant differences between the control and A30 at the 0.05 and 0.01 levels, respectively.

Compared to the control, the A30 treatment significantly elevated levels of JA-Ile (a bioactive form of JA) in young leaves (Figure 7d). In contrast, roots from the A30 treatment showed a pronounced decrease in JA, JA-Val, JA-Phe and OPDA compared to the control (Figure 7a,e–g). However, H2JA, which was present in relatively low concentrations, exhibited significantly higher accumulation in roots of the A30 treatment compared to the control (Figure 7c).

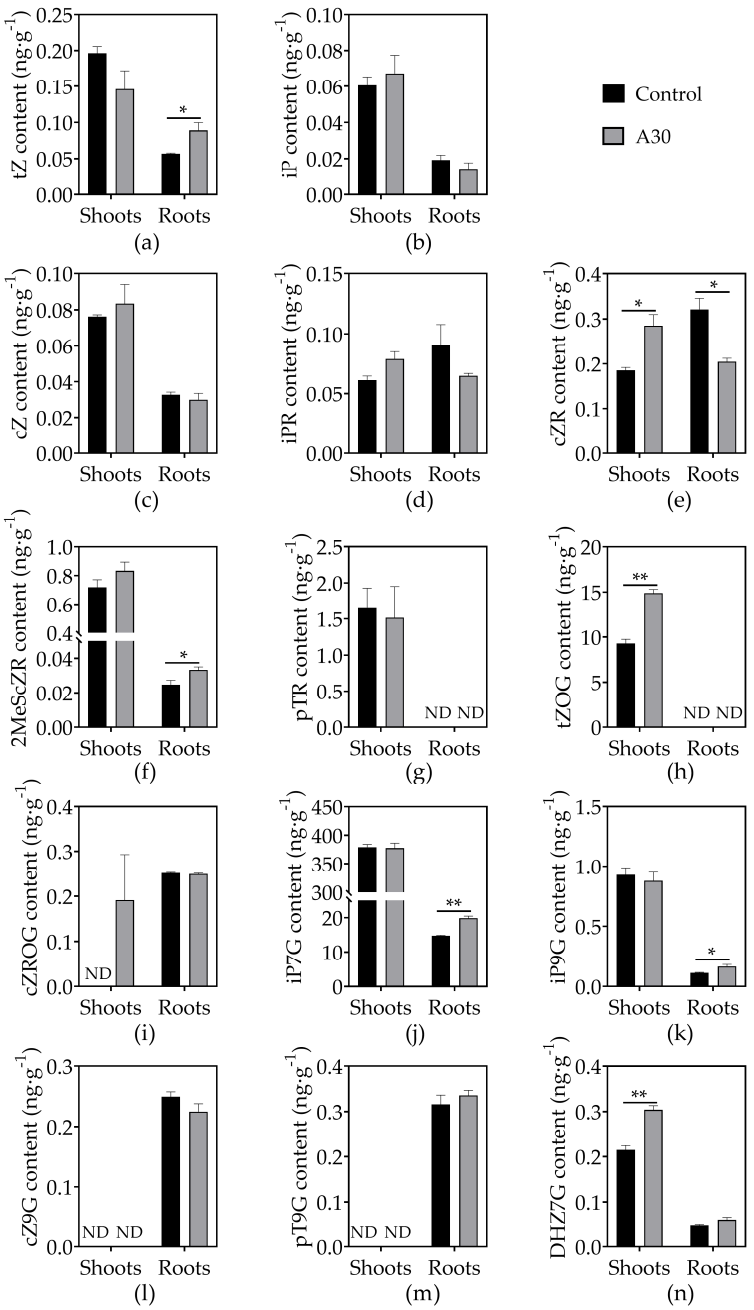


Figure 5. Contents of CKs and their derivatives in shoots and roots of tomato seedlings subjected to control and A30 treatments for 21 days. (**a**) tZ (*trans*-Zeatin) content. (**b**) iP (Isopentenyladenine) content. (**c**) cZ (*cis*-Zeatin) content. (**d**) iPR (Isopentenyladenosine) content. (**e**) cZR (cZ 9-riboside) content. (**f**) 2MeScZR (2-methylthio-cis-zeatin riboside) content. (**g**) pTR (*para*-topolin riboside) content. (**h**) tZOG (tZ O-glucoside) content. (**i**) cZROG (cZR O-glucoside) content. (**j**) iP7G (iP N7-glucoside) content. (**k**) iP9G (iP N9-glucoside) content. (**l**) cZ9G (cZ N9-glucoside) content. (**m**) pT9G (*para*-topolin-9-glucoside) content. (**n**) DHZ7G (DHZ N7-glucoside) content. Values are means ± SE (n = 3). Data were analyzed using Student's t-test (normally distributed data), or the Wilcoxon test (non-normally distributed data). ND: not detected in the samples. * and ** indicate significant differences at the 0.05 and 0.01 levels, respectively.

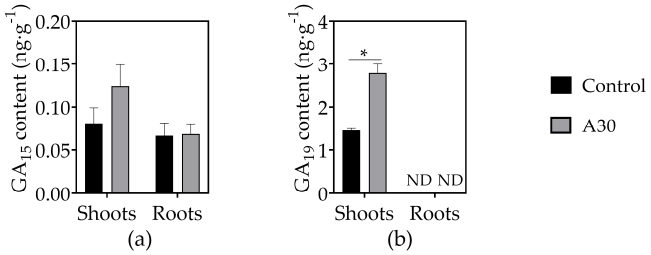


Figure 6. Contents of GA_{15} (**a**) and GA_{19} (**b**) in shoots and roots of tomato seedlings subjected to control and A30 treatments for 21 days. Values are means ± SE (n = 3). Data were analyzed using Student's t-test. Data were analyzed using Student's t-test. ND: not detected in the samples. * indicates a significant difference between the control and A30 at the 0.05 level.

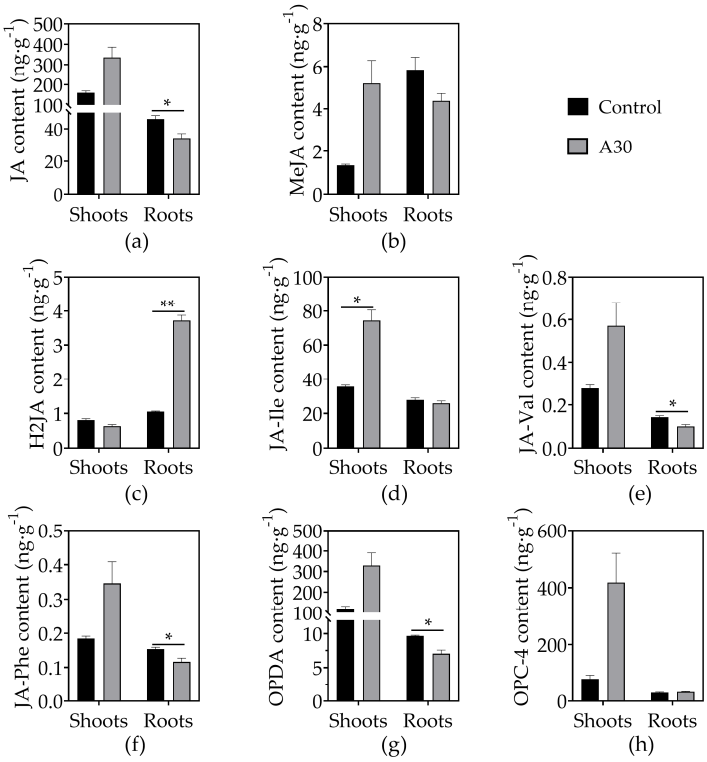


Figure 7. Contents of jasmonic acids and their derivatives in shoots and roots of tomato seedlings subjected to control and A30 treatments for 21 days. (**a**) JA (Jasmonic acid) content. (**b**) MeJA (Methyl jasmonate) content. (**c**) H2JA (Dihydrojasmonic acid) content. (**d**) JA-Ile (Jasmonoyl-L-isoleucine) content. (**e**) JA-Val (Jasmonoyl-L-valine) content. (**f**) JA-Phe (Jasmonoyl-L-phenylalanine) content. (**g**) OPDA (12-oxo-phytodienoic acid) content. (**h**) OPC-4 (3-Oxo-2-(2Z-pentenyl) cyclopentane-1-butyric acid) content. Values are means ± SE (n = 3). Data were analyzed using Student's t-test. * and ** indicate significant differences between the control and A30 at the 0.05 and 0.01 levels, respectively.

As illustrated in Figure 8a, compared to the control, the A30 treatment resulted in a non-significant reduction in leaf 1-aminocyclopropane-1-carboxylic acid (ACC) levels and a significant 39.76% increase in root ACC levels. The content of 5-deoxystrigol (5DS), a precursor of strigolactones (SLs), in shoots remained unaffected by AOS application, whereas A30 treatment significantly decreased 5DS levels in roots compared to the control.

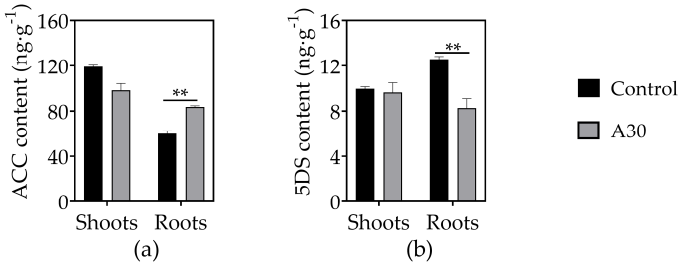


Figure 8. Contents of ACC (**a**) and 5DS (**b**) in shoots and roots of tomato seedlings subjected to control and A30 treatments for 21 days. Values are means ± SE (n = 3). Data were analyzed using Student's t-test. ** indicates a significant difference between the control and A30 at the 0.01 level.

4. Discussion

Numerous studies have documented the efficacy of AOS in enhancing plant growth performance, nutrient acquisition, metabolic activity, stress tolerance and crop productivity. In this study, AOS application enhanced chlorophyll content, photosynthetic rate and biomass in tomato seedlings, which is consistent with prior reports in other plants [7,8,15,17]. Previous studies have shown that plant growth and physiological performance exhibit a hormetic response to AOSs, characterized by stimulation at low concentrations and inhibition at higher levels, confirming a dose-dependent effect, and the optimal concentration varies among different plant species [7,9,11,14]. Under these experimental conditions, 30 mg·L^{-1} AOS yielded the highest tomato growth performance.

As the principal sites of photosynthesis, leaves generate photoassimilates that provide both structural biomass and metabolic substrates necessary for vegetative growth and reproductive output. An increased leaf area can improve light capture, thereby boosting canopy light uptake and crop photosynthesis rates, which ultimately promotes plant growth [23,24]. Additionally, studies have shown that leaf morphology significantly affects tomato fruit quality [25]. Following emergence from the shoot apical meristem, leaf primordium growth is driven by coordinated cell division and expansion. Reductions in either cell number or size result in smaller leaves [26]. This developmental progression is tightly regulated by endogenous hormones, which balance cell proliferation and expansion [27]. Notably, IAA plays a critical role in this process. Disruptions in IAA homeostasis or signaling lead to diminished leaf size [28]. Studies demonstrate that auxin activates critical growth regulators, including *ARGOS* (*Auxin Regulated Gene Involved in Organ Size*) and *SAUR* (*Small Auxin Up RNA*) genes, whose overexpression results in enlarged leaves [29,30]. GAs also play a crucial role in promoting leaf blade growth by enhancing both cell proliferation and expansion. The reduction in bioactive GA levels led to suppressed leaf expansion in tomato [31]. Genetic evidence demonstrates that GA-deficient mutants exhibit reduced leaf size, while overexpression of GA biosynthetic genes (e.g., *GA20ox1*) results in larger leaves compared to wild-type plants [32,33]. Recent studies by Li et al. [23] revealed that far-red light stimulates leaf expansion through GA metabolism regulation—upregulating *GA3ox1* and *GA20ox2* while suppressing *GA2ox5* expression, leading to increased bioactive GA accumulation. This regulatory mechanism appears conserved across species, as similar GA-mediated leaf expansion responses to environmental stimuli have been observed in tall fescue and maize [34,35]. The phytohormone CKs play a significant role in regulating leaf size. Under low red/far-red light conditions, *Arabidopsis thaliana* plants exhibit upregulated expression of *AtCKX6* (encoding CK oxidase/dehydrogenase), leading to decreased endogenous CK levels, which impairs cell proliferation capacity and inhibits leaf expansion ultimately [36]. Consistent with this finding, *AtCKX*-overexpressing transgenic plants showed significantly smaller leaves [37]. However, both CK excess and deficiency can reduce leaf size through distinct cellular mechanisms. Elevated CK levels maintain cells in

the proliferation phase, preventing the transition to cell expansion and resulting in smaller leaves. Conversely, CK deficiency suppresses cell division while promoting premature transition to cell expansion, yielding smaller leaves with significantly fewer cells [38]. In this study, the contents of IAA, CKs, and GA in tomato shoots were significantly increased by AOS treatment, which may contribute to the AOS-induced leaf expansion. The regulation of developmental processes depends not merely on the absolute levels of individual phytohormones, but more critically on their dynamic equilibrium. A prime example is the antagonistic interaction between CKs and gibberellins during leaf morphogenesis. Overexpression of *IPT7* (CK biosynthetic gene) results in enhanced tomato leaf complexity, and tomato mutants with either elevated endogenous GA content or hyperactive GA response consistently develop leaves with reduced complexity [39]. This is because CK sustains persistent morphogenetic activity at tomato leaf margins; GA exerts the opposite effect by inducing cell differentiation and thus terminating the morphogenetic phase earlier in leaf development [40].

Lateral roots are critical for the horizontal expansion of the root system to enhance nutrient and water acquisition. Their development is tightly regulated by phytohormones. Auxin plays a central role in controlling lateral root development, primarily through its biosynthesis, transport and signaling. In tomato, elevated auxin levels—whether endogenous or exogenous—promote lateral root formation [41]. Conversely, disruptions in auxin signaling or transport, either through mutations or inhibitors, impair lateral root initiation and elongation [42]. In addition, a shift from high- to low-nitrate conditions increases auxin accumulation in roots, stimulating lateral root growth [43]. However, under severe nitrogen deficiency, the nitrate transporter NRT1.1/NPF6.3 acts as an auxin transporter, reducing local auxin levels at lateral root primordia tips and suppressing lateral root emergence [44]. CKs regulate lateral root initiation by disrupting auxin gradients and inhibiting lateral root primordia formation [45]. Exogenous CK application can partially mitigate growth limitations caused by low nitrogen in *Plantago major* L. [46], which is also observed in *Arabidopsis thaliana* [47]. The balance between CKs and auxin determines root meristem size; CKs promote cell differentiation in the transition zone, whereas auxin stimulates cell division [48]. Interestingly, CK application enhances auxin biosynthesis in developing roots, while reduced CK levels decrease auxin production, highlighting their interdependent regulation [49]. JA exerts inhibitory effects on lateral root development. JAs, such as oxylipins, reduced root elongation in *Arabidopsis thaliana* [50]. Conversely, loss-of-function mutants of 9-LOX, a key enzyme in oxylipin biosynthesis, display enhanced lateral root formation, further supporting JA's inhibitory role in lateral root development [50]. SLs also negatively regulate lateral root development. Mutants of *Arabidopsis thaliana* defective in SL biosynthesis (*max3*, *max4*) or signaling (*max2*) display enhanced lateral root development compared to wild-type plants [51,52]. Ethylene generally inhibits lateral root initiation and elongation. Mutants with elevated ethylene levels and enhanced ethylene signaling (*epi*, *ctr1*, *eto1*) exhibit reduced lateral root numbers, whereas ethylene-insensitive mutants (*ein2*) show enhanced lateral root formation [53]. While ACC is a known ethylene precursor, recent studies suggest it may function independently of ethylene [54,55]. Contrary to ethylene's inhibitory effects, ACC promotes lateral root development [54]. Moreover, root development involves intricate hormonal crosstalk, with auxin serving as a central regulator. Other hormones—CKs, JA, SLs, ethylene and ACC—modulate lateral root development by interacting with auxin pathways, either synergistically or antagonistically [56]. In our study, AOS modulated hormonal homeostasis by suppressing JA and SL accumulation while promoting IAA, tZ and ACC levels, thereby orchestrating an optimal hormonal balance to enhance tomato lateral root development.

It has been proposed that oligosaccharides, including AOSs, bind to the cell membrane, thereby triggering intracellular signal transduction [5,57]. A previous study has demonstrated that AOS upregulated the expression of auxin biosynthesis- and transport-related genes in rice root cells, a process mediated by calcium signaling [17]. This study provides evidence that AOS alters the homeostasis of multiple endogenous phytohormones in tomato, potentially through transcriptional regulation of associated metabolic genes. AOSs also upregulated auxin signaling pathway genes in barley [6]. To fully understand AOS's regulatory role, further investigation is required to characterize its effects on gene expression in both metabolic and signaling pathways of phytohormones. The adoption of systems biology methodologies, particularly RNA-seq and co-expression network analysis, would be ideally suited to address this research question.

5. Conclusions

AOS exhibits a dose-dependent effect on tomato growth regulation. The concentration of 30 $mg \cdot L^{-1}$ optimally enhances chlorophyll content and photosynthetic rate, thereby increasing biomass accumulation. These findings establish AOS as a promising eco-friendly biostimulant for enhancing plant growth efficiency in protected horticulture. AOS precisely elevates endogenous levels of auxin, GA and CKs in shoots, promoting leaf expansion. Meanwhile AOS enhances lateral root development in tomato through coordinated regulation of root phytohormone profiles as follows: (1) up-regulating IAA, tZ and ACC accumulation; and (2) down-regulating JA and SL (5DS) production. Future work should integrate systems biology approaches to elucidate how AOS coordinates phytohormone metabolism and signaling to regulate plant growth.

Author Contributions: Conceptualization, L.B. and Y.L. (Yaling Li); methodology, Y.L. (Yun Li), M.S. and Y.M.; investigation, Y.L. (Yun Li), K.F. and J.W.; data curation, Y.L. (Yun Li) and L.G.; writing—original draft preparation, Y.L. (Yun Li) and J.W.; writing—review and editing, Y.L. (Yaling Li) and L.B.; funding acquisition, L.H. All authors have read and agreed to the published version of the manuscript.

Funding: This research was funded by the Shanxi Province Key R&D Plan (202102140601013, 202302010101003).

Data Availability Statement: The original contributions presented in this study are included in the article; further inquiries can be directed to the corresponding author.

Conflicts of Interest: The authors declare no conflicts of interest.

Abbreviations

The following abbreviations are used in this manuscript:

2MeScZR	2-methylthio-cis-zeatin riboside
5DS	5-deoxystrigol
ABA	Abscisic acid
ACC	1-aminocyclopropane-1-carboxylic acid
AOS	Alginate oligosaccharide
Car	Carotenoids
Chl a	Chlorophyll a
Chl b	Chlorophyll b
CK	Cytokinin
cZ	cis-Zeatin

cZ9G	cZ N9-glucoside
cZR	cZ 9-riboside
cZROG	cZR O-glucoside
DHZ7G	DHZ N7-glucoside
DM	Dry mass
GA	Gibberellic acid
H2JA	Dihydrojasmonic acid
IAA	Indole-3-acetic acid
IAA-Asp	Indole-3-acetyl-L-aspartic acid
IAA-Glc	1-O-indol-3-ylacetylglucose
IAA-Val	Indole-3-acetyl-L-valine
IAA-Val-Me	Indole-3-acetyl-L-valine
IAN	3-indoleacetonitrile
IBA	Indole-3-butyric acid
iP	Isopentenyladenine
iP7G	iP N7-glucoside
iP9G	iP N9-glucoside
iPR	Isopentenyladenosine
JA	Jasmonic acid
JA-Ile	Jasmonoyl-L-isoleucine
JA-Phe	Jasmonoyl-L-phenylalanine
JA-Val	Jasmonoyl-L-valine
MeIAA	Methyl indole-3-acetate
MeJA	Methyl jasmonate
OPC-4	3-Oxo-2-(2Z-pentenyl) cyclopentane-1-butyric acid
OPDA	12-oxo-phytodienoic acid
Pn	Net photosynthetic rate
pT9G	para-topolin-9-glucoside
pTR	para-topolin riboside
SL	Strigolactone
TAM	Tryptamine
TRP	L-tryptophan
tZ	trans-Zeatin
tZOG	tZ O-glucoside

References

1. Mostafalou, S.; Abdollahi, M. Pesticides and human chronic diseases: Evidences, mechanisms, and perspectives. *Toxicol. Appl. Pharmacol.* **2013**, *268*, 157–177. [CrossRef] [PubMed]
2. Velthof, G.L.; Lesschen, J.P.; Webb, J.; Pietrzak, S.; Miatkowski, Z.; Pinto, M.; Kros, J.; Oenema, O. The impact of the nitrates directive on nitrogen emissions from agriculture in the EU-27 during 2000–2008. *Sci. Total Environ.* **2014**, *468–469*, 1225–1233. [CrossRef]
3. Ma, Y. Does "Zero Growth Policy" affect environmental productivity of wheat production in China? *Agriculture* **2025**, *15*, 378. [CrossRef]
4. El Sheikha, A.F.; Allam, A.Y.; Taha, M.; Varzakas, T. How does the addition of biostimulants affect the growth, yield, and quality parameters of the snap bean (*Phaseolus vulgaris* L.)? How is this reflected in its nutritional value? *Appl. Sci.* **2022**, *12*, 776. [CrossRef]
5. Xing, M.; Cao, Q.; Wang, Y.; Xiao, H.; Zhao, J.; Zhang, Q.; Ji, A.; Song, S. Advances in research on the bioactivity of alginate oligosaccharides. *Mar. Drugs* **2020**, *18*, 144. [CrossRef]
6. Li, L.; Jiang, X.; Guan, H.; Wang, P. Preparation, purification and characterization of alginate oligosaccharides degraded by alginate lyase from *Pseudomonas* sp. HZJ 216. *Carbohydr. Res.* **2011**, *346*, 794–800. [CrossRef]
7. Yang, J.; Shen, Z.; Sun, Z.; Wang, P.; Jiang, X. Growth stimulation activity of alginate-derived oligosaccharides with different molecular weights and mannuronate/guluronate ratio on *Hordeum vulgare* L. *J. Plant Growth Regul.* **2021**, *40*, 91–100. [CrossRef]

8. Sarfaraz, A.; Naeem, M.; Nasir, S.; Idrees, M.; Aftab, T.; Hashmi, N.; Khan, M.M.; Moinuddin; Varshney, L. An evaluation of the effects of irradiated sodium alginate on the growth, physiological activities and essential oil production of fennel (*Foeniculum vulgare* Mill.). *J. Med. Plant Res.* **2011**, *5*, 15–21.
9. Aftab, T.; Khan, M.M.A.; Idrees, M.; Naeem, M.; Moinuddin; Hashmi, N.; Varshney, L. Enhancing the growth, photosynthetic capacity and artemisinin content in *Artemisia annua* L. by irradiated sodium alginate. *Radiat. Phys. Chem.* **2011**, *80*, 833–836. [CrossRef]
10. Naeem, M.; Idrees, M.; Aftab, T.; Khan, M.M.A.; Varshney, L. Irradiated sodium alginate improves plant growth, physiological activities and active constituents in *Mentha arvensis* L. *J. Appl. Pharm. Sci.* **2012**, *2*, 28–35. [CrossRef]
11. Ali, A.; Khan, M.M.A.; Uddin, M.; Naeem, M.; Idrees, M.; Hashmi, N.; Dar, T.A.; Varshney, L. Radiolytically depolymerized sodium alginate improves physiological activities, yield attributes and composition of essential oil of *Eucalyptus citriodora* Hook. *Carbohydr. Polym.* **2014**, *112*, 134–144. [CrossRef]
12. Moussa, H.R.; Taha, M.A.; Dessoky, E.S.; Selem, E. Exploring the perspectives of irradiated sodium alginate on molecular and physiological parameters of heavy metal stressed *Vigna radiata* L. *plants. Physiol. Mol. Biol. Plants* **2023**, *29*, 447–458. [CrossRef]
13. Zhang, Y.; Yin, H.; Wang, W.; Zhao, X.; Du, Y.; Wu, L. Enhancement in photosynthesis characteristics and phytohormones of flowering Chinese cabbage (*Brassica campestris* L. var. utilis Tsen et Lee) by exogenous alginate oligosaccharides. *J. Food Agric. Environ.* **2013**, *11*, 669–675.
14. Zhang, Y.; Liu, H.; Yin, H.; Wang, W.; Zhao, X.; Du, Y. Nitric oxide mediates alginate oligosaccharides-induced root development in wheat (*Triticum aestivum* L.). *Plant Physiol. Biochem.* **2013**, *71*, 49–56. [CrossRef]
15. Aitouguinane, M.; El Alaoui-Talibi, Z.; Rchid, H.; Fendri, I.; Abdelkafi, S.; El-Hadj, M.D.O.; Boual, Z.; Le Cerf, D.; Rihouey, C.; Gardarin, C.; et al. Elicitor Activity of low-molecular-weight alginates obtained by oxidative degradation of alginates extracted from *Sargassum muticum* and *Cystoseira myriophylloides*. *Mar. Drugs* **2023**, *21*, 301. [CrossRef] [PubMed]
16. Wang, Z.; Li, D.; Gruda, N.S.; Duan, Z.; Li, X. Fertilizer application rate and nutrient use efficiency in Chinese greenhouse vegetable production. *Resour. Conserv. Recycl.* **2024**, *203*, 107431. [CrossRef]
17. Zhang, Y.; Yin, H.; Zhao, X.; Wang, W.; Du, Y.; He, A.; Sun, K. The promoting effects of alginate oligosaccharides on root development in *Oryza sativa* L. mediated by auxin signaling. *Carbohydr. Polym.* **2014**, *113*, 446–454. [CrossRef] [PubMed]
18. Liu, H.; Zhang, Y.; Yin, H.; Wang, W.; Zhao, X.; Du, Y. Alginate oligosaccharides enhanced *Triticum aestivum* L. tolerance to drought stress. *Plant Physiol. Biochem.* **2013**, *62*, 33–40. [CrossRef]
19. Li, J.; Wang, X.; Lin, X.; Yan, G.; Liu, L.; Zheng, H.; Zhao, B.; Tang, J.; Guo, Y.-D. Alginate-derived oligosaccharides promote water stress tolerance in cucumber (*Cucumis sativus* L.). *Plant Physiol. Biochem.* **2018**, *130*, 80–88. [CrossRef] [PubMed]
20. Zhang, C.; Howlader, P.; Liu, T.; Sun, X.; Jia, X.; Zhao, X.; Shen, P.; Qin, Y.; Wang, W.; Yin, H. Alginate oligosaccharide (AOS) induced resistance to Pst DC3000 via salicylic acid-mediated signaling pathway in *Arabidopsis thaliana*. *Carbohydr. Polym.* **2019**, *225*, 115221. [CrossRef]
21. Sumanta, N.; Haque, C.I.; Nishika, J.; Suprakash, R. Spectrophotometric analysis of chlorophylls and carotenoids from commonly grown fern species by using various extracting solvents. *Res. J. Chem. Sci.* **2014**, *4*, 63–69.
22. Liu, J.; Yang, J.; Jiang, C.; Zhou, J.; Zhao, Y.; Huang, L. Volatile organic compound and endogenous phytohormone characteristics during callus browning in *Aquilaria sinensis*. *Ind. Crops Prod.* **2021**, *168*, 113605. [CrossRef]
23. Li, S.; Ran, S.; Yuan, S.; Chang, K.; Han, M.; Zhong, F. Gibberellin-mediated far-red light-induced leaf expansion in cucumber seedlings. *Protoplasma* **2024**, *261*, 571–579. [CrossRef] [PubMed]
24. Kalaitzoglou, P.; van Ieperen, W.; Harbinson, J.; van der Meer, M.; Martinakos, S.; Weerheim, K.; Nicole, C.C.S.; Marcelis, L.F.M. Effects of continuous or end-of-day far-red light on tomato plant growth, morphology, light absorption, and fruit production. *Front. Plant Sci.* **2019**, *10*, 322. [CrossRef]
25. Rowland, S.D.; Zumstein, K.; Nakayama, H.; Cheng, Z.; Flores, A.M.; Chitwood, D.H.; Maloof, J.N.; Sinha, N.R. Leaf shape is a predictor of fruit quality and cultivar performance in tomato. *New Phytol.* **2020**, *226*, 851–865. [CrossRef]
26. Horiguchi, G.; Ferjani, A.; Fujikura, U.; Tsukaya, H. Coordination of cell proliferation and cell expansion in the control of leaf size in *Arabidopsis thaliana*. *J. Plant Res.* **2006**, *119*, 37–42. [CrossRef]
27. Alabadí, D.; Blázquez, M.A. Molecular interactions between light and hormone signaling to control plant growth. *Plant Mol. Biol.* **2009**, *69*, 409–417. [CrossRef]
28. Saini, K.; Markakis, M.N.; Zdanio, M.; Balcerowicz, D.M.; Beeckman, T.; De Veylder, L.; Prinsen, E.; Beemster, G.T.S.; Vissenberg, K. Alteration in auxin homeostasis and signaling by overexpression of PINOID kinase causes leaf growth defects in *Arabidopsis thaliana*. *Front. Plant Sci.* **2017**, *8*, 1009. [CrossRef]
29. Rai, M.I.; Wang, X.; Thibault, D.M.; Kim, H.J.; Bombyk, M.M.; Binder, B.M.; Shakeel, S.N.; Schaller, G.E. The *ARGOS* gene family functions in a negative feedback loop to desensitize plants to ethylene. *BMC Plant Biol.* **2015**, *15*, 157. [CrossRef]
30. Spartz, A.K.; Lee, S.H.; Wenger, J.P.; Gonzalez, N.; Itoh, H.; Inzé, D.; Peer, W.A.; Murphy, A.S.; Overvoorde, P.J.; Gray, W.M. The *SAUR19* subfamily of *SMALL AUXIN UP RNA* genes promote cell expansion. *Plant J.* **2012**, *70*, 978–990. [CrossRef]

31. Shohat, H.; Ceriker, H.; Vasuki, H.; Illouz-Eliaz, N.; Blum, S.; Amsellem, Z.; Tarkowska, D.; Aharoni, A.; Eshed, Y.; Weiss, D. Inhibition of gibberellin accumulation by water deficiency promotes fast and long-term 'drought avoidance' responses in tomato. *New Phytol.* **2021**, *232*, 1985–1998. [CrossRef] [PubMed]
32. Ueguchi-Tanaka, M.; Nakajima, M.; Katoh, E.; Ohmiya, H.; Asano, K.; Saji, S.; Hongyu, X.; Ashikari, M.; Kitano, H.; Yamaguchi, I.; et al. Molecular interactions of a soluble gibberellin receptor, GID1, with a rice DELLA protein, SLR1, and gibberellin. *Plant Cell* **2007**, *19*, 2140–2155. [CrossRef]
33. Wang, H.; Jiang, H.; Xu, Y.; Wang, Y.; Zhu, L.; Yu, X.; Kong, F.; Zhou, C.; Han, L. Systematic analysis of gibberellin pathway components in *Medicago truncatula* reveals the potential application of gibberellin in biomass improvement. *Int. J. Mol. Sci.* **2020**, *21*, 7180. [CrossRef]
34. Xu, Q.; Burgess, P.; Xu, J.; Meyer, W.; Huang, B. Osmotic stress- and salt stress-inhibition and gibberellin-mitigation of leaf elongation associated with up-regulation of genes controlling cell expansion. *Environ. Exp. Bot.* **2016**, *131*, 101–109. [CrossRef]
35. Mu, X.; Chen, Q.; Wu, X.; Chen, F.; Yuan, L.; Mi, G. Gibberellins synthesis is involved in the reduction of cell flux and elemental growth rate in maize leaf under low nitrogen supply. *Environ. Exp. Bot.* **2018**, *150*, 198–208. [CrossRef]
36. Carabelli, M.; Possenti, M.; Sessa, G.; Ciolfi, A.; Sassi, M.; Morelli, G.; Ruberti, I. Canopy shade causes a rapid and transient arrest in leaf development through auxin-induced cytokinin oxidase activity. *Genes. Dev.* **2007**, *21*, 1863–1868. [CrossRef]
37. Raspor, M.; Motyka, V.; Žižková, E.; Dobrev, P.I.; Trávníčková, A.; Zdravković-Korać, S.; Simonović, A.; Ninković, S.; Dragićević, I.C. Cytokinin profiles of *AtCKX2*-overexpressing potato plants and the impact of altered cytokinin homeostasis on tuberization in vitro. *J. Plant Growth Regul.* **2012**, *31*, 460–470. [CrossRef]
38. Skalák, J.; Vercruyssen, L.; Claeys, H.; Hradilová, J.; Černý, M.; Novák, O.; Plačková, L.; Saiz-Fernández, I.; Skaláková, P.; Coppens, F.; et al. Multifaceted activity of cytokinin in leaf development shapes its size and structure in Arabidopsis. *Plant J.* **2019**, *97*, 805–824. [CrossRef]
39. Shwartz, I.; Levy, M.; Ori, N.; Bar, M. Hormones in tomato leaf development. *Dev. Biol.* **2016**, *419*, 132–142. [CrossRef]
40. Nakayama, H.; Ichihashi, Y.; Kimura, S. Diversity of tomato leaf form provides novel insights into breeding. *Breed. Sci.* **2023**, *73*, 76–85. [CrossRef]
41. Negi, S.; Sukumar, P.; Liu, X.; Cohen, J.D.; Muday, G.K. Genetic dissection of the role of ethylene in regulating auxin-dependent lateral and adventitious root formation in tomato. *Plant J.* **2010**, *61*, 3–15. [CrossRef]
42. Laskowski, M.; Grieneisen, V.A.; Hofhuis, H.; Hove, C.A.T.; Hogeweg, P.; Marée, A.F.M.; Scheres, B. Root system architecture from coupling cell shape to auxin transport. *PLoS Biol.* **2008**, *6*, e307. [CrossRef] [PubMed]
43. Ötvös, K.; Marconi, M.; Vega, A.; O'Brien, J.; Johnson, A.; Abualia, R.; Antonielli, L.; Montesinos, J.C.; Zhang, Y.; Tan, S.; et al. Modulation of plant root growth by nitrogen source-defined regulation of polar auxin transport. *EMBO J.* **2021**, *40*, e106862. [CrossRef]
44. Asim, M.; Ullah, Z.; Oluwaseun, A.; Wang, Q.; Liu, H. Signalling overlaps between nitrate and auxin in regulation of the root system architecture: Insights from the *Arabidopsis thaliana*. *Int. J. Mol. Sci.* **2020**, *21*, 2880. [CrossRef] [PubMed]
45. Ahmad, N.; Jiang, Z.; Zhang, L.; Hussain, I.; Yang, X. Insights on phytohormonal crosstalk in plant response to nitrogen stress: A focus on plant root growth and development. *Int. J. Mol. Sci.* **2023**, *24*, 3631. [CrossRef]
46. Zaman, M.; Kurepin, L.V.; Catto, W.; Pharis, R.P. Enhancing crop yield with the use of N-based fertilizers co-applied with plant hormones or growth regulators. *J. Sci. Food Agric.* **2015**, *95*, 1777–1785. [CrossRef]
47. Kiba, T.; Kudo, T.; Kojima, M.; Sakakibara, H. Hormonal control of nitrogen acquisition: Roles of auxin, abscisic acid, and cytokinin. *J. Exp. Bot.* **2011**, *62*, 1399–1409. [CrossRef]
48. Dello Ioio, R.; Linhares, F.S.; Scacchi, E.; Casamitjana-Martinez, E.; Heidstra, R.; Costantino, P.; Sabatini, S. Cytokinins determine *Arabidopsis* root-meristem size by controlling cell differentiation. *Curr. Biol.* **2007**, *17*, 678–682. [CrossRef]
49. Jones, B.; Gunnerås, S.A.; Petersson, S.V.; Tarkowski, P.; Graham, N.; May, S.; Dolezal, K.; Sandberg, G.; Ljung, K. Cytokinin regulation of auxin synthesis in *Arabidopsis* involves a homeostatic feedback loop regulated via auxin and cytokinin signal transduction. *Plant Cell* **2010**, *22*, 2956–2969. [CrossRef]
50. Vellosillo, T.; Martínez, M.; López, M.A.; Vicente, J.; Cascón, T.; Dolan, L.; Hamberg, M.; Castresana, C. Oxylipins produced by the 9-lipoxygenase pathway in *Arabidopsis* regulate lateral root development and defense responses through a specific signaling cascade. *Plant Cell* **2007**, *19*, 831–846. [CrossRef]
51. Kapulnik, Y.; Delaux, P.-M.; Resnick, N.; Mayzlish-Gati, E.; Wininger, S.; Bhattacharya, C.; Séjalon-Delmas, N.; Combier, J.-P.; Bécard, G.; Belausov, E.; et al. Strigolactones affect lateral root formation and root-hair elongation in *Arabidopsis*. *Planta* **2011**, *233*, 209–216. [CrossRef]
52. Ruyter-Spira, C.; Kohlen, W.; Charnikhova, T.; van Zeijl, A.; van Bezouwen, L.; de Ruijter, N.; Cardoso, C.; Lopez-Raez, J.A.; Matusova, R.; Bours, R.; et al. Physiological effects of the synthetic strigolactone analog *gr24* on root system architecture in Arabidopsis: Another belowground role for strigolactones? *Plant Physiol.* **2011**, *155*, 721–734. [CrossRef] [PubMed]
53. Negi, S.; Ivanchenko, M.G.; Muday, G.K. Ethylene regulates lateral root formation and auxin transport in *Arabidopsis thaliana*. *Plant J.* **2008**, *55*, 175–187. [CrossRef]

54. Mou, W.; Khare, R.; Polko, J.K.; Taylor, I.; Xu, J.; Xue, D.; Benfey, P.; Van de Poel, B.; Chang, C.; Kieber, J.J. Ethylene-independent modulation of root development by ACC via downregulation of WOX5 and group I CLE peptide expression. *Proc. Natl. Acad. Sci. USA* **2025**, *122*, e2417735122. [CrossRef]
55. Mou, W.; Kao, Y.-T.; Michard, E.; Simon, A.A.; Li, D.; Wudick, M.M.; Lizzio, M.A.; Feijó, J.A.; Chang, C. Ethylene-independent signaling by the ethylene precursor ACC in *Arabidopsis* ovular pollen tube attraction. *Nat. Commun.* **2020**, *11*, 4082. [CrossRef]
56. Saini, S.; Sharma, I.; Kaur, N.; Pati, P.K. Auxin: A master regulator in plant root development. *Plant Cell Rep.* **2013**, *32*, 741–757. [CrossRef] [PubMed]
57. Larskaya, I.A.; Gorshkova, T.A. Plant oligosaccharides—Outsiders among elicitors? *Biochemistry* **2015**, *80*, 881–900. [CrossRef]

Disclaimer/Publisher's Note: The statements, opinions and data contained in all publications are solely those of the individual author(s) and contributor(s) and not of MDPI and/or the editor(s). MDPI and/or the editor(s) disclaim responsibility for any injury to people or property resulting from any ideas, methods, instructions or products referred to in the content.